

Machine learning techniques in a structural and functional MRI diagnostic approach in schizophrenia: a systematic review

This article was published in the following Dove Press journal:
Neuropsychiatric Disease and Treatment

Renato de Filippis^{1,*}
Elvira Anna Carbone^{1,*}
Raffaele Gaetano¹
Antonella Bruni¹
Valentina Pugliese¹
Cristina Segura-Garcia²
Pasquale De Fazio¹

¹Department of Health Sciences, University Magna Graecia of Catanzaro, Catanzaro 88100, Italy; ²Department of Medical and Surgical Sciences, University Magna Graecia of Catanzaro, Catanzaro 88100, Italy

*These authors contributed equally to this work

Background: Diagnosis of schizophrenia (SCZ) is made exclusively clinically, since specific biomarkers that can predict the disease accurately remain unknown. Machine learning (ML) represents a promising approach that could support clinicians in the diagnosis of mental disorders.

Objectives: A systematic review, according to the PRISMA statement, was conducted to evaluate its accuracy to distinguish SCZ patients from healthy controls.

Methods: We systematically searched PubMed, Embase, MEDLINE, PsychINFO and the Cochrane Library through December 2018 using generic terms for ML techniques and SCZ without language or time restriction. Thirty-five studies were included in this review: eight of them used structural neuroimaging, twenty-six used functional neuroimaging and one both, with a minimum accuracy >60% (most of them 75–90%). Sensitivity, Specificity and accuracy were extracted from each publication or obtained directly from authors.

Results: Support vector machine, the most frequent technique, if associated with other ML techniques achieved accuracy close to 100%. The prefrontal and temporal cortices appeared to be the most useful brain regions for the diagnosis of SCZ. ML analysis can efficiently detect significantly altered brain connectivity in patients with SCZ (eg, default mode network, visual network, sensorimotor network, frontoparietal network and salience network).

Conclusion: The greater accuracy demonstrated by these predictive models and the new models resulting from the integration of multiple ML techniques will be increasingly decisive for early diagnosis and evaluation of the treatment response and to establish the prognosis of patients with SCZ. To achieve a real benefit for patients, the future challenge is to reach an accurate diagnosis not only through clinical evaluation but also with the aid of ML algorithms.

Keywords: machine learning, schizophrenia, support vector machine, resting-state fMRI, sMRI, multivariate pattern analysis

Introduction

Schizophrenia (SCZ) is a major psychiatric disorder characterized by delusions and hallucinations with a loss of contact with reality (so-called positive symptoms), flat affect, anhedonia, loss of motivation (avolition), poor speech (alogia), social withdrawal (so-called negative symptoms) and cognitive impairment, which have a strong impact on the patient and society.¹ The average incidence is 15.2 per 100,000 people, the lifetime prevalence is 0.40% and the pooled male–female rate ratio is 1.4.² A recent review estimated that approximately 1 in 200 individuals will

Correspondence: Pasquale De Fazio
Psychiatry Unit, Department of Health Sciences, University Magna Graecia of Catanzaro, Viale Europa, Italy Via Broussard 13, Catanzaro 88100, Italy
Tel/Fax +39 096 171 2393
Email defazio@unicz.it

be diagnosed with SCZ at some point during their lifetime, with variations based on the geographic region.³ Diagnosis is based on the Diagnostic and Statistical Manual of Mental Disorders 5 (DSM-5)⁴ or on the ICD⁵ and is exclusively clinical, since specific biomarkers that can predict the illness accurately remain unknown.⁶ Pattern recognition methods applied to neuroimaging data represent a new and promising approach that could support clinicians in the diagnosis of mental disorders.⁷ Magnetic resonance imaging (MRI) is today one of the most used techniques for the study of the neurobiological bases of SCZ. Computerized methods are necessary to analyze large amounts of imaging data with great precision. The most relevant information is extracted from the images, and then a model classification method is able to process this information in order to determine the probability of disease.⁸ The new approach is exemplified by the application of machine learning (ML) techniques such as support vector machines (SVM), a high-dimensional, pattern recognition, supervised learning algorithm⁹ or multivariate pattern analysis (MVPA) or the random forest (RF). These techniques are most useful when analyzing highly complex datasets to enable the discovery of relationships that are not evident from simple statistics and thus to make accurate predictions based on these statistics.¹⁰

This research seeks to evaluate the evidence about the role of ML techniques in making diagnostic discrimination in SCZ during the last 30 years. To the best of our knowledge, there are no systematic reviews investigating these features. We aimed to provide a comprehensive systematic review according to the PRISMA statement¹¹ of different ML techniques used to distinguish SCZ patients from healthy controls (HC). It was not our goal to catalog all methods of ML, to report on applications of ML in psychiatry nor to explain or illustrate any particular method in detail.

Materials and methods

Search strategy

We searched PubMed, Embase, MEDLINE, PsychINFO and the Cochrane Library for articles published up to December 31, 2018, without language and time restriction, by using the following keywords: (“Big data” OR “Artificial Intelligence” OR “Machine Learning” OR “Gaussian process” OR “Cross-validation” OR “Cross validation” OR “Crossvalidation” OR “Regularized logistic” OR “Linear discriminant analysis” OR “LDA” OR “Random forest”

OR “Naïve Bayes” OR “Least Absolute selection shrinkage operator” OR “elastic net” OR “LASSO” OR “RVM” OR “relevance vector machine” OR “pattern recognition” OR “Computational Intelligence” OR “Machine Intelligence” OR “Knowledge Representation” OR “Knowledge Representations” OR “support vector” OR “SVM” OR “Pattern classification” OR “Deep learning”) AND (“Schizophrenia”). Two authors reviewed all the selected studies independently. The reference lists were screened to find additional data. The eligible publications have been included and cited in this review. This systematic review was developed according to the PRISMA statement.¹¹

Assessment of study quality

The Jadad rating system¹² was applied to check the methodological quality of studies in this systematic review. Jadad’s procedure enables qualification of a study according to the clarity in describing the randomization, the double-blinding procedure and the withdrawal and dropout reports. Score ranges from 0 to 5. For this systematic review, the inclusion criteria was a Jadad score >3.

Selection criteria

We included studies using ML techniques with schizophrenic patients diagnosed according to the DSM-IV, DSM IV-TR, DSM-5 or ICD-10 criteria. These patients could have chronic SCZ or be diagnosed with a first episode of schizophrenia (FES) and could be drug-naïve or under antipsychotic treatment. We excluded studies with patients who exhibited general medical, neurological or psychiatric comorbidity, substance abuse or alcohol dependence, traumatic brain injuries with loss of consciousness or unclear or unverified diagnoses according to the DSM or ICD criteria. Studies without control groups were also excluded.

Data collection, extraction and statistical analysis

Two researchers (EAC and RdF) independently screened the titles and abstracts of the identified articles and read the full texts of articles that met the eligibility criteria, supervised by RG, who made the final decision in cases of disagreement. Article data included year of publication, ML model and algorithm (eg, SVM, MVPA, RF), sample size, diagnoses assessed in the study and statistical data (ie, accuracy, sensitivity, specificity, area under the ROC curve [AUC]).

Results

Initially, 2,386 items were identified, of which 2,215 articles were excluded because they did not fulfill inclusion criteria. The abstracts of the remaining 171 articles were reviewed. In all, 60/171 articles were deleted because they were editorials, letters to editors, reviews, meta-analyses, case reports or different interventions. Then, 76 manuscripts of 111 papers were deleted because they did not fulfill the criteria for inclusion, while the remaining 35 were included. Of the latter, 8 used structural neuroimaging and 26 used functional neuroimaging and 1 both (Figure 1).

Eight studies used structural magnetic resonance imaging (sMRI) in order to distinguish patients with SCZ or adolescent-onset schizophrenia (AOS) or FES from patients with other psychiatric disorders (eg, bipolar disorder (BD), major depressive disorder (MDD)) or HC (Table 1). In particular, many of these studies focused on differences between grey matter (GM) and white matter (WM).

Twenty-six studies used functional magnetic resonance imaging (fMRI) to achieve the same goal (Table 2). They

evaluated abnormalities in brain functional connectivity (FC) parameters (regional homogeneity (ReHo), density), networks or the entire functional connectome.

Only one study used both structural and fMRI.

Structural neuroimaging

Salvador et al combined and compared the most common ML methods (ridge, Least Absolute Shrinkage and Selection Operator (LASSO), elastic net and L_0 norm regularized logistic regression, a support vector classifier, regularized discriminant analysis, RF and a Gaussian process classifier) in a sample of 128 SCZ, 128 BD and 127 HC. They used different features: GM and WM voxel-based morphometry (VBM), vertex-based cortical thickness and volume, set as region of interest (ROI), and volumetric measures and wavelet-based morphometry as inputs for the techniques. VBM is the feature of choice for sMRI and it shows the most accuracy in distinguishing patients from HC, whilst the other ML methods (eg, ridge, LASSO, a support vector classifier, RFs and a Gaussian

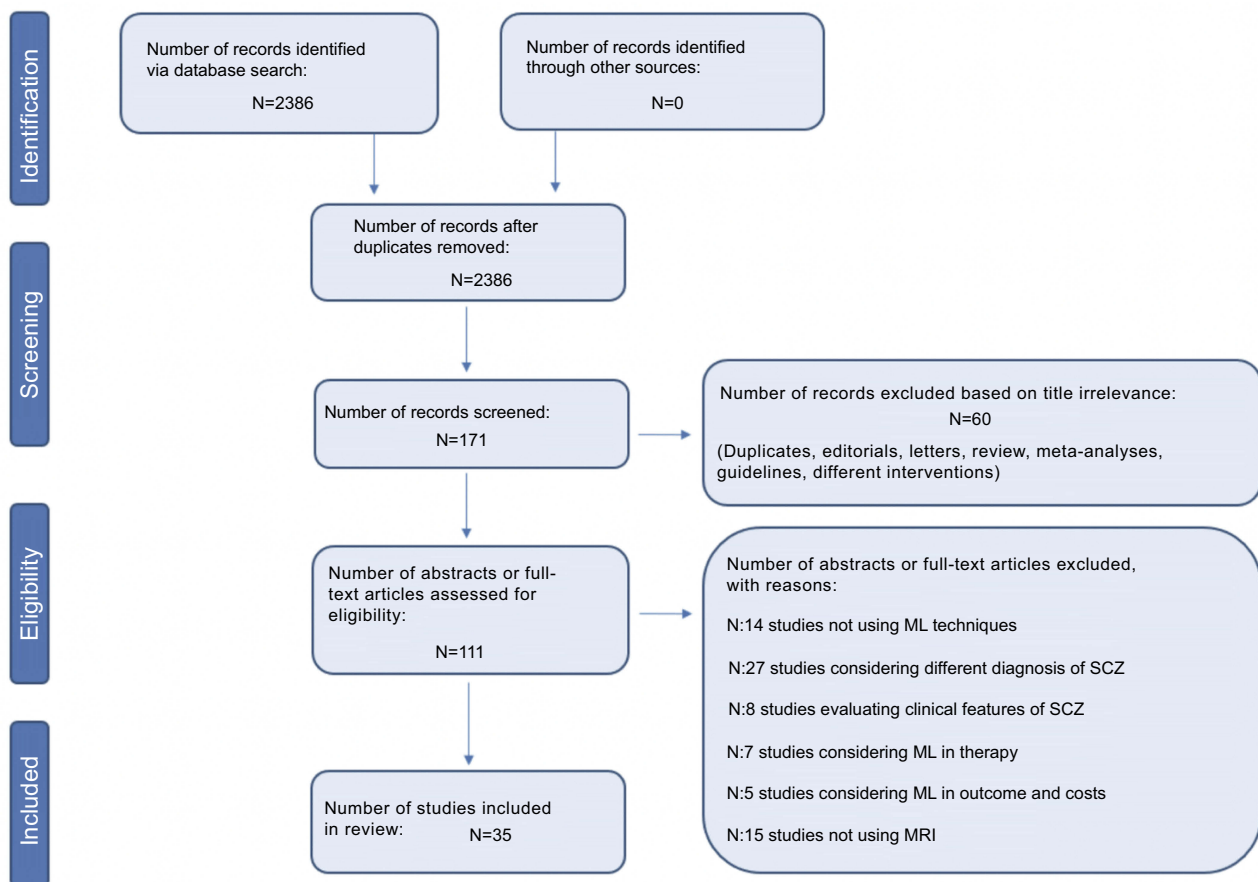


Figure 1 PRISMA flow diagram of included studies.

Table 1 Summary of included studies of machine learning techniques classifying schizophrenia using structural neuroimaging

First author, Year	Data utilized	Sample size and diagnosis	Machine learning model	Best accuracy (%)	Other measures (sensitivity, specificity, AUC, precision, error rate)	Data features	Brain regions and networks involved	Commentary
Greenstein, 2012 ¹⁷	sMRI 1.5T	197 subjects: -98 Childhood onset SCZ -99 HC	RF	73.7%	N.A.	Cortical thickness for 68 frontal, temporal, parietal, and occipital lobe regions, and bilateral lateral ventricle, thalamus, and hippocampus volumes to yield the 74 variables authors used as features	Left temporal lobes, bilateral dorsolateral prefrontal regions and left medial parietal lobes.	Authors have chosen to use regional brain measures that provide lower resolution compared to the higher resolution voxel-wise measures
Castellani, 2012 ¹⁵	sMRI 1.5T	108 subjects: -54 SCZ -54 HC	SVM	66.4–84.1%	N.A.	Landmark point detection of DLPFC and Feature vocabulary	Dorsolateral prefrontal cortex	Findings may have partially been limited by administration of AP or by length of illness
Iwabuchi, 2013 ²⁰	sMRI 3T and 7T	39 subjects: -19 SCZ -20 HC	SVM	GM 3T 66.6% 7T 77% WM 3T 63.9% 7T 69.1%	Sn 63.2% Sp 70.0% Sn 78.9% Sp 75% Sn 57.9% Sp 70.0% Sn 63.2% Sp 75.0%	The normalized, modulated, unsmoothed WM, and GM images for the 3- and 7-T datasets were then used as inputs to the separate linear SVM classifiers	Insula, anterior cingulate cortex, thalamus, superior temporal cortex, parahippocampal gyrus	First study compares head-to-head GM and WM in SVM analysis
Lu, 2016 ¹⁴	sMRI 3T	83 subjects: -41 SCZ -42 HC	SVM RFE	SVM-RFE, 88.4%	Sn 91.9% Sp 84.4%	First, RGMV and RWMV in the VBM analysis; second, the significant between-group differences for both RGMV and RWMV by the ROI analysis as the input features for the classifier	Middle occipital gyrus, calcarine, cuneus, fusiform gyrus, lingual gyrus, hippocampus, parahippocampal gyrus	Chronic SCZ patients brain structures might be affected by antipsychotic use

(Continued)

Table 1 (Continued).

First author, Year	Data utilized	Sample size and diagnosis	Machine learning model	Best accuracy (%)	Other measures (sensitivity, specificity, AUC, precision, error rate)	Data features	Brain regions and networks involved	Commentary
Pinaya, 2016 ¹⁸	sMRI 1.5T	258 subjects: -143 SCZ -32 FEP -83 HC	DBN-DNN SVM	DBN-DNN, 73.6% ±6.84	Sn 76.4% ±0.1 Sp 70.7% ±12.2 Error rate 26.1 ±6.5	Sixty-eight brain regions (thirty-four in each hemisphere) and volumes of the forty-five anatomical structures	Frontal, temporal, parietal and insular cortices, corpus callosum, putamen, cerebellum.	They classified HC and SCZ; FEP as third classification on a continuum between HC and SCZ
Xiao, 2017 ¹⁶	sMRI 3T	326 subjects: -163 Drug-naïve FES -163 HC	SVM	surface area 85.0% cortical thickness 81.8%	Sn 83.0% Sp 87.0% Sn 76.9% Sp 85.0%	The cortical thickness and surface area features of 68 cortical regions from the Desikan atlas were extracted: frontal, temporal, parietal, and occipital lobe regions	Left fusiform, lingual, posterior cingulate, supramarginal, insula, inferior parietal, rostral anterior cingulate, rostral middle frontal AND right isthmus cingulate, lateral occipital, lingual, caudal middle frontal, inferior parietal, frontal and temporal pole cortex	Most of interested areas belong to the DMN, salience network or visual system
Salvador, 2017 ¹³	sMRI 1.5T	383 subjects: -128 SCZ -128 BD -127 HC	Ridge LASSO SVC RF GPC Elastic Net L ₀	74–77% (SCZ vs HC)	N.A.	Cortical thickness of left and right hemispheres; Cortical volume of left and right hemispheres; Grey and White matter voxel based morphometry (VBM) images; Grey and White matter wavelet based morphometry (VBM) images	Cortical thickness, Cortical volume, Grey and White matter	Multi-class classifications considering all groups at the same time have made high predictive power for the SCZ group

(Continued)

Table 1 (Continued).

First author, Year	Data utilized	Sample size and diagnosis	Machine learning model	Best accuracy (%)	Other measures (sensitivity, specificity, AUC, precision, error rate)	Data features	Brain regions and networks involved	Commentary
Amin, 2018 ⁴⁷	sMRI 3T T1-weighted	298 subjects: -144 SCZ -154 HC	Translation-based multi-modal fusion approach	N.A.	N.A.	dFNC as the functional features and ICA-based sources from gray matter densities as the structural features	Putamen, insular; precuneus, posterior cingulate cortex and temporal cortex	The deep learning approach has a potential for learning dynamic features from the fMRI data, and thus can offer a favorable framework for multimodal fusion in the brain imaging research.
Pinaya, 2019 ¹⁹	sMRI	75 subjects: -40 HC -35 SCZ	Deep auto-encoder	N.A.	Mean deviation metric of 1,14 ±0.28	Cortical cortical thickness of the 68 cortical subregions (34 per hemisphere) and the anatomical structural volume of 36 structures; total number: 104	Left ventral diencephalon, left choroid plexus, left lateral ventricle, right cuneus, right superior temporal, left putamen, right lateral ventricle, left cerebellum cortex, left precentral.	The model was also able to detect distinct patterns of neuroanatomical deviations in SCZ. The deep autoencoder can be used to measure the overall deviation metric of an individual and elucidate which regions are the most different compared to healthy group.

Note: For this systematic review the inclusion criteria was a Jaded score >3.

Abbreviations: AOS, adolescent-onset schizophrenia; ASD, autism spectrum disorder; AUC, area under ROC curve; DBN, deep belief network; dFNC, dynamic functional connectivity; DLPFC, dorsolateral prefrontal cortex; DNN, deep neural network; eMIC, extended maximal information coefficient; FEP, first episode psychosis; fMRI, functional magnetic resonance imaging; GM, gray matter; GPC, Gaussian process classifiers; GSM, generalized sparse model; HC, healthy control; LDA, linear discriminant analysis; LIBSVM, leave-one-out SVM; LOOCV, leave-one-out cross validation; MDD, major depressive disorder; ML, machine learning; MPPA, multivariate pattern analysis; L₀, L₁ norm regularization; LASSO, Least Absolute Shrinkage and Selection Operator; N.A., not applicable; PCC, Pearson correlation coefficient; RF, random forest; RGMV, regional gray matter volume; RFE, recursive feature elimination; ROC, receiver-operating characteristic curve analysis; ROI, region of interest; rsfMRI, resting state magnetic resonance imaging; RVMV, regional white matter volume; SCZ, schizophrenia; sMRI, structural magnetic resonance imaging; Sn, sensitivity; SNPs, single-nucleotide polymorphisms; Sp, specificity; SRVS, sparse-representation-based variable selection; SVC, support vector classifier; SVM, support vector machine; T, tesla; VBM, voxel-based morphometry; v-ELM, voting-ELM; v-MKL, multiple kernel learning; VMHC, voxel-mirrored homotopic connectivity; WBM, wavelet-based morphometry; WM, white matter.

Table 2 Summary of included studies of Machine Learning techniques classifying Schizophrenia using functional neuroimaging

First author, Year	Data utilized	Sample size and diagnosis	Machine learning model	Best accuracy (%)	Other measures (sensitivity, specificity, AUC, precision, error rate)	Data features	Brain regions and networks involved	Commentary
Yoon, 2008 ²⁴	fMRI 1.5T	34 subjects: -19 SCZ -15 HC	MVPA	93%	N.A.	Images were acquired with a echo-planar imaging (EP) in the anterior commissure- posterior commissure (AC-PC) aligned axial plane. Twenty-seven interleaved slices for whole-brain coverage were collected with a 22-cm field of view	Prefrontal Cortex, sensory cortex, visual cortex	Accuracy of MVPA was higher for HC group
Yang, 2010 ³³	fMRI 3T SNPs Combined fMRI-SNPs	40 subjects: -20 SCZ -20 HC	SVM-E/C Hybrid ML method	SVM-C 67, 5% Hybrid ML 87, 3%	SVM-C Sn 65% Sp 70% Hybrid ML Sn 85, 8% Sp 88.8%	150 SNPs from a database; auditory stimuli were used and found to be effective in eliciting fMRI BOLD patterns differentiating HC from SZ subjects	Post-/pre-central gyrus, paracentral lobule, cingulate gyrus, superior and inferior parietal lobule, precuneus	Hybrid ML method using fMRI and SNP data
Su, 2013 ³⁹	fMRI 1.5T	64 subjects: -32 SCZ -32 HC	SVM	MIC 76, 6% PCC 81, 2% eMIC 82, 8%	MIC Sn 71, 9% Sp 81, 2% PCC Sn 81, 2% Sp 81, 2% eMIC Sn 81, 2% Sp 84, 4%	180 registered fMRI volumes with the MNI template than further divided into 116 regions according to the automatic anatomical labelling atlas. The atlas divides the cerebrum into 90 regions (45 in each hemisphere) and divides the cerebellum into 26 regions (nine in each cerebellar hemisphere and eight in the vermis)	Default mode network, cerebellum, visual network, sensorimotor network, frontoparietal network, cingulo-opercular network	The study does not include definition of ROIs and it is confined to connectivity analyses

(Continued)

Table 2 (Continued).

First author, Year	Data utilized	Sample size and diagnosis	Machine learning model	Best accuracy (%)	Other measures (sensitivity, specificity, AUC, precision, error rate)	Data features	Brain regions and networks involved	Commentary
Zhu, 2014 ³¹	rs-fMRI 3T	45 subjects: -27 SCZ -28 HC	LOOCV	83.6%	Sn 81.5% Sp 85.7%	Blood oxygen level-dependent (BOLD) time courses were generated for 23 regions of interest (ROIs)	Wernicke's area, inferior parietal, Broca's area, pars triangularis, middle frontal, pars opercularis, orbitals, inferior temporal, superior frontal, caudate, putamen, ventral thalamus, cerebellum crus, striate, extrastriate, posterior, superior parietal, superior temporale, cingulate.	Authors propose an adaptive learning algorithm to distinguish HC and SCZ patients using resting-state functional language network
Castro, 2014 ⁴³	fMRI	52 subjects: -31 SCZ -21 HC	v-MKL	85%	Sn 90% Sp 76%	Authors used the simulation toolbox for fMRI data (SimTB) mimics the BOLD response of subjects. The experimental design is characterized by the absence of task events. Among the 30 components available by default on SimTB, they did not include in the simulation those associated with the visual cortex, the precentral and postcentral gyri, the subcortical nuclei and the hippocampus	Right Caudate Nucleus, precuneus, cingulate gyrus, occipital, gyrus, parietal lobe and left precuneus, temporal gyrus, parahippocampal gyrus, paracentral lobule	All patients were on stable medication prior to the scan session
Arbabshirani, 2014 ³⁴	fMRI 3T	370 subjects: -195 SCZ -175 HC	SVM	88, 2%	Sn 86, 7% Sp 89, 5%	47 ICNs were selected, resulting in 1081 FNC features for each subject: in total we extracted 1128 features for each subject	Subcortical, auditory, visual, somatomotor regions and control processes, default-mode, cerebellar networks	The study evaluates functional network connectivity and autoconnectivity improving the classification performance significantly

(Continued)

Table 2 (Continued).

First author, Year	Data utilized	Sample size and diagnosis	Machine learning model	Best accuracy (%)	Other measures (sensitivity, specificity, AUC, precision, error rate)	Data features	Brain regions and networks involved	Commentary
Watanabe, 2014 ³⁸	rs-fMRI	91 subjects: -54 SCZ -67 HC	SVM LASSO Graph Net Elastic Net ROC	77–88.2%	N.A.	Authors produced a whole-brain resting state functional connectome. 347 non-overlapping spherical nodes are placed throughout the entire brain in a regularly-spaced grid pattern; each of these nodes represents a pseudo-spherical ROI. For each of these nodes, a single representative time-series is assigned by spatially averaging the BOLD signals falling within the ROI	Intra-frontoparietal, frontoparietal-default, intracerebellum networks, lateral prefrontal cortex	Authors introduced empirical risk minimization framework that accounts for 6-D spatial structure in the connectome via the fused LASSO and Graph Net regularizer
Cao, 2014 ³²	fMRI 1.5-3T SNPs	208 subjects: -92 SCZ -116 HC	SRVS GSM	SNPs 83.1% ± 1.3 fMRI 63.1% ± 0.7	N.A.	SNPs/fMRI voxels (n=759,075/153,594. For each method, authors carried out 100 runs and the average of the classification ratios was used as the final identification accuracy	Temporal lobe, lateral frontal lobe, occipital lobe, motor cortex.	Different nature of the data used for the ML analysis
Maturaba, 2015 ³⁶	rs-fMRI	211 subjects: -48 SCZ -46 BD -117 HC	DGM	76.6%	Sn 58.5% Sp 84.9%	Authors parcellated each fMRI image into 116 ROIs using an automated anatomical labeling template. The data of subjects whose fMRI images did not match the template even after the spatial normalization were also discarded	Left and right thalamus, left fusiform, right rectus, right middle cingulum, right supra-marginal, left mild temporal, left superior orbital frontal, left superior temporal, right caudate	The DGM was a generative model implemented using deep neural networks

(Continued)

Table 2 (Continued).

First author, Year	Data utilized	Sample size and diagnosis	Machine learning model	Best accuracy (%)	Other measures (sensitivity, specificity, AUC, precision, error rate)	Data features	Brain regions and networks involved	Commentary
Koch, 2015 ²³	fMRI 1.5T	98 subjects: -44 SCZ -54 HC	MVPA SVM ROC LIBSVM	69.3–93.2%	Sn 70.5–100% Sp 40.9–93.2%	Gradient-echo echo-planar imaging was used to produce eighteen slices approximately parallel to the AC-PC plane, covering the inferior part of the frontal lobe (superior border above the caudate nucleus), the entire temporal lobe, and large parts of the occipital region. Six fMRI volumes were acquired per trial, resulting in 450 volumes per run	Ventral striatum, right pallidum, putamen, right inferior frontal gyrus, nucleus accumbens, amygdala, insula, thalamus, inferior temporal gyrus	Seven patients taking atypical AP. 21 typical AP and 16 not receiving any medications
Chyzyk, 2015 ³⁰	rs-fMRI	147 subjects: -72 SCZ -75 HC	V-ELM SVM RF	VMHC ≈90%	N.A.	rs-fMRI data was collected with single-shot full k-space EPI with ramp sampling correction using the AC-PC as a reference. The first 6 volumes were discarded for scanner calibration leaving 144 time volumes	Inferior temporal gyrus, parahippocampalgyrus, planumpolare, temporal fusiform cortex, thalamus	Application of SVM and RF to the features extracted from cross-validation as the ensembles of ELM

(Continued)

Table 2 (Continued).

First author, Year	Data utilized	Sample size and diagnosis	Machine learning model	Best accuracy (%)	Other measures (sensitivity, specificity, AUC, precision, error rate)	Data features	Brain regions and networks involved	Commentary
Cabral, 2016 ²¹	rs-fMRI sMRI	145 subjects: -71 SCZ -74 HC	MVPA	rs-fMRI 70.5% sMRI 69.7% s/rs-fMRI 75%	GM, Sn 82.4% Sp 63.4% acc. 69.7% RS, Sn 71.2% Sp 69.7% rs-fMRI, Sn 100% Sp 62.5–87.5% acc. 76.9–92.3% MRI, Sn 75% Sp 78.8% acc. 71.2%	sMRI data were preprocessed to segment the brain into WM, GM, and cerebral spinal fluid. Blood oxygenation level dependent images of the whole brain using an EPI sequence were acquired in 32 axial slices using the AC-PC plane as a reference. RS scans resulted in 304 seconds duration (152 volumes). After discarding the first 10 images and 2 dummy scans, the remaining 140 images were unwarped	Fronto-occipital, fronto-parietal, fronto-temporal, cortico-thalamic regions, left inferior temporal gyrus, parahippocampal gyrus	The AP medication at MRI scan was converted to chlorpromazine and olanzapine equivalents; chronic effects of AP could contribute to alterate FC with longer duration of illness
Kim, 2016 ³⁷	rs-fMRI 3T	100 subjects: -50 SCZ -50 HC	DNN		Error rate of DNN: 14.2% vs error rate of SVM: 22.3%.	Authors acquired 150 volumes. The first 5 volumes were removed to allow equilibration of the T1-related signal. Each of the 116 AAL regions was readily available in each voxel of the normalized EPI volumes	Whole-brain FC patterns	The study successfully demonstrated the feasibility of the DNN classifier toward the automated diagnosis of SZ patients
Liu, 2017 ²⁹	rs-fMRI 3T	79 subjects: -48 Drug-naïve SCZ -31 HC	SVM	89.9%	Sn 91.67% Sp 87.10%	For each subject, the fMRI scan lasted for 480s, and 240 volumes were obtained. The first 10 volumes of each subject were discarded to certain steady-state conditions	Left postcentral gyrus, left superior temporal gyrus, left paracentral lobule, right precentral gyrus, right inferior parietal lobule, right middle frontal gyrus, bilateral precuneus	Study includes only AOS without SCZ patients

(Continued)

Table 2 (Continued).

First author, Year	Data utilized	Sample size and diagnosis	Machine learning model	Best accuracy (%)	Other measures (sensitivity, specificity, AUC, precision, error rate)	Data features	Brain regions and networks involved	Commentary
Guo, 2017 ²⁷	fMRI short/long-range FCs	96 subjects: -28 SCZ -40 HC -28 relatives	SVM ROC	94.6%	Sn 92.9% Sp 96.4%	Long-range and short-range FCs. rs-fMRI images were obtained with a gradient-echo echo-planar imaging sequence using 250 volumes	Default-mode network, sensorimotor circuits, right superior parietal lobule, left fusiform gyrus, cerebellum	The results may be confounded by acute positive symptoms since the patients sample was unmedicated and recent onset
Orban, 2017 ⁴⁵	fMRI	382 subjects: -191 SCZ -191 HC	SVM	84%	N.A.	Functional brain connectomes included 2016 functional connections between 64 brain parcels	Whole brain connectivity	Brain imaging data from 6 independent studies and datasets
Wang, 2017 ²⁸	rs-fMRI 3T	79 subjects: -48 AOS -31 HC	SVM	90.1%	Sn 88.2% Sp 91.9%	Brain regions with significantly different ReHo values between patients with AOS and healthy controls	Bilateral superior medial prefrontal cortex, left superior temporal gyrus, right precentral lobule, right inferior parietal lobule, left paracentral lobule	Different number of participants in the two groups. with AOS (with less confounding factors) instead of SCZ
Chen, 2017 ²²	rs-fMRI 3T	60 subjects: -20 SCZ -20 MDD -20 HC	MVPA	85% SCZ vs MDD (average 79%)	Sn 98% Sp 60%	The scan used a gradient-echo echo-planar imaging sequence. A total of 255 volumes were collected for each subject. Each functional volume contained 35 slices. To minimize the effects of scanner signal stabilization, the first five volumes of each subject were excluded from all analyses	Orbitofrontal cortex	The systematically different medications for SCZ and MDD may have different effects on functional connectivity; the medicated patients were in stable condition and this may have an impact on the functional connectivity of cortical networks

(Continued)

Table 2 (Continued).

First author, Year	Data utilized	Sample size and diagnosis	Machine learning model	Best accuracy (%)	Other measures (sensitivity, specificity, AUC, precision, error rate)	Data features	Brain regions and networks involved	Commentary
Wang, 2017 ²⁶	rs-fMRI 3T	79 subjects: -48 drug-naïve AOS -31 HC	SVM FC analysis LIBSVM ROC	92.4%	Sn 89.6% Sp 96.8%	Authors used regional homogeneity (ReHo), a measurement that reflects brain local functional connectivity or synchronization and indicates regional integration of information processing	Right middle frontal gyrus, right superior medial prefrontal cortex, left superior temporal gyrus	SVM analysis applied to an independent dataset
Bae, 2017 ⁴⁰	fMRI 3T	75 subjects: -21 SCZ -54 HC	SVM	92.1%±10.5	Sn 92.0±15.8% Sp 92.1±8.1% Precision 94±6.3%	Authors created anatomic labels for 90 ROIs from the image database. Any subject with fewer than 85 ROIs automatically labeled was excluded	Anterior right cingulate cortex, superior right temporal region, inferior left parietal region	Possible influence of pharmacological treatment and disease stage on the investigated functional connections, they used only n-back tests without rs-fMRI
Qureshi, 2017 ⁴⁴	rs-fMRI 3T	144 subjects: -72 SCZ -72 HC	ELM SVM LDA RF	99.3%	Sn 100% Sp 98, 6%	Authors used measures including the mean cortical thickness, cortical thickness standard deviation, surface area, volume, mean curvature, white matter volume, subcortical segment volume, subcortical intensity, and overall brain volume and intensity as the structural features	Cortical thickness, Surface area, WM/subcortical/overall volume, curvature, global average functional connectivity	Authors developed an ELM, whose effectiveness was compared with that of more known ML methods

(Continued)

Table 2 (Continued).

First author, Year	Data utilized	Sample size and diagnosis	Machine learning model	Best accuracy (%)	Other measures (sensitivity, specificity, AUC, precision, error rate)	Data features	Brain regions and networks involved	Commentary
Reavis, 2017 ²⁵	fMRI 3T	148 subjects: -50 SCZ -51 BD -47 HC	MVPA	41%	N.A.	Structural data were processed and parcellated into anatomical regions used to constrain ROI definitions	Lateral occipital lobe	The paper shows MVPA can be used successfully to classify individual perceptual stimuli in SCZ and BD. The results do not provide group differences with utilized stimuli
Chen, 2017 ³⁵	rs-fMRI	109 subjects: -35 SCZ -31 HC -22 ASD -21 HC	MVPA LOOCV	Schizophrenia, 83% ASD, 80.4%	SCZ, Sn 80% Sp 87.1% AUC 0.83 ASD, Sn 77.27% Sp 83.23% AUC 0.76	A total of 255 volumes were collected for each subject. Each functional volume contained 35 slices. The first five volumes of each subject were excluded from all analyses. Only the brain areas within the areas identified in the MVPA were included in the subsequent analyses. They were regarded as meaningful brain areas and used as ROIs in the functional connectivity analysis	Default-mode network, salience network	The two datasets were from two different imaging platforms
Pläschke, 2017 ⁴¹	rs-fMRI	170 subjects: -86 SCZ -84 HC	SVM	61–72%	Sn 65–77% Sp 46–69% AUC 0.61–0.79	Authors investigated 12 functional networks. Only meta-analytic networks with a minimum of 10 nodes were included, since a lower number of features are uninformative for robust classification	Emotion-processing, empathy and cognitive action control networks	Young-old classification was based on all networks and outperformed clinical classification

(Continued)

Table 2 (Continued).

First author, Year	Data utilized	Sample size and diagnosis	Machine learning model	Best accuracy (%)	Other measures (sensitivity, specificity, AUC, precision, error rate)	Data features	Brain regions and networks involved	Commentary
Liu, 2018 ⁴²	rs-fMRI	79 subjects: -48 Drug-Naive FES AOS -31 HC	SVM VMHC	94.93%	Sn 100% Sp 87.09%	For each subject, the fMRI scan lasted for 480 s, and 240 volumes were obtained. The first 10 volumes of each subject were discarded to certain steady-state conditions and for participants to acclimatize to a scanning environment during the analyzed portion of the data	Fusiform gyrus, superior temporal gyrus, insula, precentral gyrus and precuneus	authors also used a battery of neurocognitive tests and they demonstrated deficits in multiple cognitive functions in patients
Zeng, 2018 ⁴⁶	rs-fMRI 1.5-3T	734 subjects: -357 SCZ -377 HC	RFE-SVM RFE-LDA SAN DANS	81–85%	Sn 75–83% Sp 81–86%	Authors used multi-atlas based whole-brain fMRI in the MVPA, which measures functional connectivity of the same image in different spaces. The three atlases used included 176, 160 and 116 ROIs respectively	Cortical-striatal-cerebellar circuit (default, salience, frontoparietal control, ventral attention, dorsal attention and somatomotor, visual).	This paper provides for a multi-variate based whole-brain fMRI pattern analysis to ensure the optimal use of the wealth of information present in fMRI scans.
Amin, 2018 ⁴⁷	fMRI 3T T2-weighted	298 subjects: -144 SCZ -154 HC	Translation-based multimodal fusion approach	N.A.	N.A.	dFNC as the functional features and ICA-based sources from grey matter densities as the structural features	Putamen, insular, precuneus, posterior cingulate cortex and temporal cortex	The deep learning approach has a potential for learning dynamic features from the fMRI data, and thus can offer a favorable framework for multimodal fusion in the brain imaging research.

Note: For this systematic review the inclusion criteria was a Jaded score >3.

Abbreviations: AC-PC plane, bicommissural plane; AOS, adolescent-onset schizophrenia; ASD, autism spectrum disorder; AUC, area under ROC curve, Cohe-ReHo, regional homogeneity based on coherence; DANS, discriminant autoencoder network with sparsity constraint; DBN, Deep Belief Network; DNN, deep neural network; dFNC, dynamic functional connectivity; DGM, deep neural generative model; eMIC, extended maximal information coefficient; EPI, echo-planar imaging; FC, functional connectivity; FEP, first episode psychosis; fMRI, functional magnetic resonance imaging; GM, grey matter; GPC, Gaussian process classifiers; GSM, generalized sparse model; HC, healthy control; ICNs, intrinsic connectivity networks; LDA, linear discriminant analysis; LIBSVM, leave-one-out SVM; LOOCV, leave-one-out cross validation; MDD, major depressive disorder; ML, machine learning; MVPA, multivariate pattern analysis; L0, L0 norm regularization; LASSO, Least Absolute Shrinkage and Selection Operator; N.A., not applicable; PCC, Pearson correlation coefficient; ReHo, regional homogeneity; RF, random forest; RFE, recursive feature elimination; ROC, receiver-operating characteristic curve analysis; ROI, region of interest; rsfMRI, resting state magnetic resonance imaging; SAN, sparse autoencoder network; SCZ, schizophrenia; sMRI, structural magnetic resonance imaging; Sn, sensitivity; SimTB, simulation toolbox for fMRI data; SNP, single-nucleotide polymorphisms; Sp, specificity; SRVS, sparse-representation-based variable selection; SVC, support vector classifier; SVM, support vector machine; T, tesla; v-ELM, voting-ELM; v-MKL, multiple kernel learning; VMHC, voxel-mirrored homotopic connectivity; WM, white matter.

process classifier) have similar and lower performance levels.¹³

The grey matter volume (GMV) and WM volume of 41 SCZ patients and 42 HC were compared through a ML method providing both SVM and recursive feature elimination. Important abnormalities in brain structures primarily involved in cognitive functions (eg, memory, emotionality) were identified with 88.4% accuracy (sensitivity 91.9%, specificity 84.4%). The authors concluded with the possibility of identifying specific brain neuroimaging profiles associated with SCZ as a potential biomarker for disease diagnosis.¹⁴

The dorsolateral prefrontal cortex (DLPFC) was chosen as the ROI in another study. The ROI-SVM approach was used to classify 54 SCZ patients and 54 HC with accuracy (left side 75%; right side 66.38%). The technique showed better results among females and older subjects, probably due to differences in GM distribution (left side 84.09%, right side 77.27% for females and left side 81.25%, right side 70.83% for seniors). According to the authors, DLPFC can be used as a brain structural marker for the disease, especially in older female chronic patients.¹⁵

Patterns of illness-related grey matter changes could be potential biomarker for identifying structural brain alterations in individuals with SCZ. Xiao et al used SVM to analyze cortical thickness and surface area measurements in the differentiation of 163 FES patients and 163 HC. Regions contributing to classification accuracy included the grey matter in default mode network (DMN), central executive network, salience network (SN) and visual network: left fusiform, lingual, posterior cingulate, supramarginal, insula and right isthmus cingulate, lateral occipital, lingual and frontal pole cortex. The accuracy of correct classification of patients and HC was 85.0% for surface area and 81.8% for cortical thickness.¹⁶

The RF method with 74 anatomic brain MRI subregions was used to classify 98 childhood-onset SCZ patients and 99 HC. The association of copy number variations and these 74 subregions in the RF produced 74% accuracy. The brain areas specifically involved were the left temporal lobe, bilateral dorsolateral prefrontal region and left medial parietal lobe.¹⁷

Pinaya et al developed a new deep learning model, named the Deep Belief Network, used for extrapolating and interpreting features from neuromorphometry data on 83 HC and 143 patients with SCZ. Deep Belief Network accuracy, utilized as SVM was 68.1%, whereas as

a classifier it was 73.6%, detecting large differences between classes, especially for frontal, temporal, parietal and insular cortices and the corpus callosum, putamen and cerebellum.¹⁸

In a later study, it was proposed an alternative conceptual and practical approach for investigating brain-based disorders that not requires a large number of cases. They used an artificial neural network known as “deep autoencoder” to create a normative model using sMRI data. The model was able to generate different values of total neuroanatomical deviation and distinct patterns of neuroanatomical deviations.¹⁹

Finally, pathologic changes both in WM and GM (in bilateral insula, anterior cingulate cortex, thalamus, superior temporal cortex and parahippocampal gyrus) were demonstrated though SVM. Changes were more evident at 7T RMI rather than at 3T RMI; the accuracy was higher with 7T in discriminating patients from controls (77% vs 66%) (20 HC vs 19 SCZ).²⁰

Functional neuroimaging

Cabral et al applied MVPA to both structural and functional magnetic resonance neuroimaging methods on 21 SCZ patients and 74 HC. The resting state fMRI (rs-fMRI) reported similar accuracy to the structural classifier (70.5% vs 69.7%, respectively). The combination of sMRI and rs-fMRI outperformed single MRI modalities by reaching 75% accuracy. Subcortical short-range, in particular inter-hemispheric connections, were the main aberrant connections identified in SCZ patients. Abnormalities found in the frontotemporal area could explain cognitive impairment (eg, reduced verbal fluency, negative symptoms).²¹

Chen et al used rs-fMRI to compare three groups (20 SCZ, 20 MDD and 20 HC) through local FC density analysis combined with MVPA. Based on this method, they could differentiate MDD patients from SCZ patients according to the local FC density value in the orbitofrontal cortex; in fact, the connection in the prefrontal cortex was significantly lower in patients with SCZ compared with other groups (accuracy 85%). These findings emphasize the great importance the prefrontal cortex may have in future ML studies attempting to improve the diagnosis of SCZ by differentiating it from other pathological conditions such as MDD. A limitation of the study could be the enrolment of patients who were in a chronic phase and receiving pharmacological treatment, which could alter FC.²²

Koch et al reached 93% accuracy in identifying SCZ patients through the MPVA analysis of patterns of

anticipation of a monetary reward. They studied the frontal, temporal, occipital and midbrain regions, with a peak in the right pallidum and claimed to predict the severity of the negative symptoms of patients based on ventricular striatal activation patterns. Therefore, they conclude that such ML methods could bring significant benefits to diagnostic classification based on fMRI signal patterns.²³

Yoon et al enrolled a sample of 19 SCZ and 15 HC and tried to decode the specific neural networks activated in the recognition and classification of stimuli. Two cycles of stimuli including faces, scenes, objects and scrambled images were presented to participants. Functional MRI data were analyzed through MVPA. The authors' hypothesis about an alteration in brain connections in SCZ patients was confirmed: patients were less accurate than HC (59% vs 72%, respectively); moreover, the distributed representations of visual objects were compromised in SCZ. In both groups, the accuracy of the classification was significantly correlated with behavioral measures. This impairment was directly correlated with a decrease in performance in the 1-back matching task. Patterns of cortical activity (prefrontal, sensory and visual cortex) are reflected in altered behavior. The authors pointed out that the impairment emerging from fMRI data could reflect the neural abnormalities at the basis of poor performance in the matching task.²⁴

Reavis et al showed four different objects and an outdoor scene to 51 BD patients, 50 SCZ patients and 31 HC during the execution of a fMRI and then performed a MVPA classification analysis to assess the distinctiveness of activity corresponding to the perception of each stimulus in the lateral occipital complex. As the authors did not find differences between groups (accuracy 41%), they hypothesized that if a deficit exists, it is linked to specific categories of objects (not between-group but within-group differences).²⁵

In a recent paper, Wang et al explored long- and short-range functional connectivity (IFC) (sFC) through rs-fMRI in 48 first-episode, drug-naïve AOS patients and 31 HC using SVM. They found abnormalities of lpFC and spFC in some brain networks (both lpFC and spFC increased in the anterior DMN and decreased in the posterior DMN and lpFC only decreased in the SN). They were able to classify patients and controls with high accuracy (up to 92.4%), sensitivity (89.6%) and specificity (96.8%). This study was the first to examine IFC and sFC in the whole brain in first-episode drug-naïve AOS patients through rs-fMRI. The authors concluded that the functional alterations could point to a role of DMN and SN in the neurobiology of

SCZ that is already present in patients in the first episode, hence their ability to discriminate AOS patients from HC with great diagnostic accuracy.²⁶

Another paper published by Guo et al²⁷ also examined the role of s-IFCs in fMRI in differentiating patients from HC or their own relatives. Specifically, SCZ patients showed an increase in spFC and lpFC in the DMN, while, unlike in the previous manuscript, they both decreased in sensorimotor circuits. In addition, the combination of spFC values in the right superior parietal lobule and lpFC in the left fusiform cerebellum gyrus was able to differentiate patients from their relatives with an adequate level of sensitivity and specificity. Wang et al enrolled 49 drug-naïve AOS patients and 32 HC to investigate and identify brain abnormalities using ReHo input in SVM analysis through rs-fMRI. The study found that AOS patients showed significantly increased ReHo values in the bilateral superior medial prefrontal cortex and decreased ReHo values in the left superior temporal gyrus, right precentral lobule, right inferior parietal lobule, and left paracentral lobule compared with HC.²⁸

Liu et al used a similar sample with 48 AOS and 31 HC to analyze the coherence regional homogeneity (CoHe-ReHo) through ML methods with rs-fMRI. The CoHe-ReHo value was reduced in the left postcentral gyrus, left superior temporal gyrus, left paracentral lobule, right precentral gyrus, right IPL, right middle frontal gyrus and bilateral praecuneus. It did not appear to increase in any cerebral area in AOS patients compared with HC.²⁹

Chyzyk et al used the amplitude of low-frequency fluctuations, fractional ALFF, voxel-mirrored homotopic connectivity (VMHC) and ReHo as input data for voting-ELM (v-ELM) (SVM+RF) analysis. The accuracy of this method proved to be close to 90%. The study compared 72 SCZ patients and 75 HC. The anatomic brain regions with major alterations were the inferior temporal gyrus, anterior division of the parahippocampal gyrus, planum polare, temporal fusiform cortex and left and right thalamus.³⁰

Zhu et al developed a new method named the "Adaptive Learning Algorithm" to distinguish 27 SCZ patients from 28 HC using rs-fMRI data. They identified 23 ROI of the resting-state functional language network that are considered important in language comprehension and production (eg, Wernicke's area, Broca's area, inferior parietal, inferior temporal). They reached an accuracy of 83.6%, a sensitivity of 81.5% and a specificity of 85.7%.³¹

Cao et al integrated fMRI data with single-nucleotide polymorphisms (SNPs) in their research with 92 SCZ

patients and 116 HC. This type of ML analysis represents a challenge for the future, given the unique nature of the data used. Therefore, the authors have specially developed a new sparse-representation-based variable selection (SRVS) algorithm, which can identify the most significant biomarker elements associated with SCZ. The accuracy obtained by the investigators through the SRVS algorithm was significantly greater than those obtained by the single methods with the traditional statistical methods: SNPs alone can reach an identification accuracy of approximately $83.11\% \pm 1.32\%$, while the accuracy of top fMRI voxels alone was $63.13\% \pm 0.74\%$. This demonstrates the importance of an integrated analysis using biomarkers from different types of biological sources (eg, fMRI, SNP) to improve the capacity to distinguish SCZ patients from HC.³²

Yang et al used a hybrid ML model combining fMRI and SNPs data (combined SNP-fMRI) with an accuracy of 87%. The study sample consisted of 20 SCZ patients and 20 HC. They identified 150 SNPs, 15 of which were located in 14 important genes (eg, COMT, DISC1, MTHFR, HTR3B, GAD2, SLC6A4, ABCB1 and ABCC). The brain regions that better classified SCZ patients and HC resulted to be the inferior, middle and medial frontal gyri, cingulate gyrus, superior temporal gyrus and praecuneus.³³

Instead, Arbabshirani et al proposed another method to discriminate 195 SCZ from 175 HC that provided extrapolation data from rs-fMRI of two different types of features: functional network connectivity (FNC) to capture the internetwork connectivity pattern and autoconnectivity to capture the temporal connectivity of each brain network. The combination of these features (FNC+autoconnectivity) with the SVM method allowed them to achieve a diagnostic and classification accuracy of 88.21% (83.7% FNC alone and 80.2% autoconnectivity alone), a 86.7% sensitivity (81.4% FNC alone and 78.1% autoconnectivity alone) and an 89.5% specificity (85.9% FNC alone and 82.2% autoconnectivity alone).³⁴

A recent study examined 35 FES teenagers, 31 HC and 22 people with autism spectrum disorder (ASD). The SVM classification showed an accuracy of 83.33% (sensitivity of 80%, specificity 87.1%, AUC 0.83). The authors claimed that shared atypical brain connections in the DMN and SN, useful for distinguishing SCZ patients from HC, were also detected in the ASD group. Such functional connections present in both groups of patients but not in the HC may help us to better understand the pathogenetic

and etiological mechanisms of the disorders.³⁵ A ML-based method of diagnosing SCZ using a deep neural generative model (DGM) of rs-fMRI images was proposed by Matsubara et al. The proposed DGM achieved a good diagnostic accuracy (76,6%), sensitivity (58,5%) and specificity (84,9%). It can also measure the contribution weight of each brain region to the diagnosis: right and left thalamus appeared to be the regions that can most accurately differentiate patients from HC.³⁶

Another study successfully demonstrated the feasibility and the minimum error rate of the deep neural network-classifier toward the automated diagnosis of SCZ patients by using resting-state whole-brain FC patterns as input.³⁷ They found different FC patterns useful for distinguishing SCZ from HC. The whole-brain FC data suggest that such approaches show improved ability to learn hidden patterns in brain imaging data, which may be useful for a better understanding of the neural basis and for developing diagnostic tools for SCZ identifying associated aberrant FC patterns.

Watanabe et al produced a whole-brain resting-state functional connectome. The final dataset included 67 HC and 54 SCZ patients. They assessed three sets of network-to-network connections (intra-frontoparietal, frontoparietal default, intra-cerebellar) as they were considered to be of major importance in the psychopathology of SCZ. The final accuracy rate ranged from 77% of LASSO to 88.2% of LASSO fused. This is one of the first studies to evaluate the entire connectivity of both HC and SCZ patients, identifying major network alterations.³⁸ Su L. et al rebuilt the entire functional brain connectivity of SCZ patients by using fMRI and matched it with that of HC. Pearson correlation coefficient, maximal information coefficient and extended maximal information coefficient resulted in three main FC types. They applied MVPA to discriminate these three types of functional models evaluating the power of nonlinear rather than linear FC in 32 SCZ patients and 32 HC and determined the spatial distribution of brain regions related to symptomatology. They achieved >80% accuracy and found that nonlinear FC was increased in SCZ patients; this shows that this variable has an equal, if not greater, impact on the diagnostic classification of SCZ.³⁹ On the other hand, Bae et al used a fMRI public dataset and extrapolated the FC parameters. The results showed a reduction in the global and local network connectivity in subjects affected by SCZ (n=21) compared with HC (n=54), particularly in the anterior right

cingulate cortex, the superior right temporal region and the inferior left parietal region. The accuracy was 92.1% using SVM and 10-fold cross-validation (sensitivity 92%, specificity 92.1%, precision 94%); this suggests important and significant differences regarding the regional brain activity through fMRI in both groups. The aim of their work was to demonstrate that brain connectivity was significantly altered in patients with SCZ compared with HC and that these differences could be efficiently and more easily detected by ML analysis.⁴⁰

Pläschke et al used SVM classification and distinguished with 68% accuracy (AUC, 0.73) SCZ patients from matched HC basing on resting-state FC. The networks that distinguished patients most accurately from HC were emotional scenes and face processing, empathic processing and cognitive action control. It was the first study that took into account the age of the participants in the classification: classification based on age was excellent based on all networks. Resting-state FC could be used as a marker of functional dysregulation in specific network affected in SCZ; the age, in fact, affects network integrity in a more global way.⁴¹

The alteration in FC in different brain region was also studied by Liu et al in a sample of 48 drug-naïve, first-episode, AOS and 31 HC. In order to discriminate patients from controls, they combined the VMHC values in the precentral gyrus and precuneus performing rs-fMRI. They found that patients with AOS showed dysfunctional inter-hemispheric cooperation within the sensorimotor network. It was correlated with processing speed deficits, indicating that this dysfunction may contribute to cognitive deficits in patients. The SVM analysis showed sensitivity of 100%, specificity of 87.09%, and accuracy of 94.93%.⁴²

Castro et al aimed to develop an improved variant of the algorithm of normal multiple kernel learning (MKL) capable of analyzing a greater variety of brain region patterns to improve the current SCZ diagnosis accuracy. The participants followed a three-stimulus auditory odd-ball discrimination task, in which two runs of 244 auditory stimuli consisting of standard, target and novel stimuli were presented to the subject. This technique (v-MKL) is able to find an automatic combination of kernel functions that can be applied to multiple data sources (both magnitude and phase fMRI data) and adds an additional 5% to the accuracy of the standard MKL (85%).⁴³

Qureshi et al developed an extreme learning machine (ELM), whose effectiveness was compared with that of more known ML methods, reaching a maximum accuracy

of 99.3%. They enrolled 72 patients with SCZ and 72 HC using a new hybrid weighted function concatenation method to gain the highest precision that maintained a high discriminatory power through the weight of the individual characteristic type. The most interesting data extrapolated from the acquisitions were cortical thickness and surface area, total cerebral volume, WM volume, intensity measures from the cortical parcellation, volume and intensity from sub-cortical parcellation and overall volume of cortex features. Then, a permutation test was performed to evaluate the statistical weight of the results obtained by the new method. The conclusion was that this ELM technique can be used in clinical practice and offers a concrete possibility of helping clinicians to diagnose SCZ.⁴⁴

The research of Orban et al, with nearly 200 patients and 200 HC, represents one of the largest ML studies on SCZ to date. The authors reported 84% diagnostic accuracy using data from multiple sites, while significantly lower accuracy was achieved with the use of individual sites. In fact, when data from all subjects and sites were gathered together, an association analysis at the level of all components revealed a decrease in connectivity in patients with SCZ. Univariate mass analyses demonstrated a cerebral disconnection through the entire brain with identifiable alterations in over a third of brain connections from cognitive to primary sensory networks.⁴⁵

In a recent paper, Zeng et al collected data from seven imaging resources (for a total of 357 SCZ patients and 377 controls) using a multi-atlas based whole-brain fcMRI in the multivariate pattern analysis, which measures FC of the same image in different spaces of multiple atlases. This large multi-site fMRI study developed a deep discriminant autoencoder network with sparsity constraint (DANS) network with multi-atlas fcMRI to discriminate SCZ patients from HC. The high accuracy achieved (81–85%) suggests the potential of discriminant deep learning of multi-atlas fcMRI in searching biomarkers to achieve clinical diagnosis of SCZ across multiple independent imaging sites.⁴⁶

Finally, Amin et al proposed a novel translation-based fusion model that learns “alignments” (or links) between brain structure and function. The authors considered two different imaging views of the same brain like two different languages conveying some common facts that enable finding linkages between dynamic functional connectivity (dFNC) features from fMRI data and static GM patterns from sMRI data. The dFNC states characterized by weakly correlated intrinsic connectivity networks (ICNs) were

found to have stronger association with putamen and insular GM pattern, while the dFNC states of profuse strongly correlated ICNs exhibited stronger links with the GM pattern in precuneus, posterior cingulate cortex and temporal cortex.⁴⁷

Discussion

ML techniques represent a promising approach that could support clinicians in the diagnosis of mental disorders and may be useful in classifying SCZ through MRI. All studies included in the review achieved a minimum accuracy of approximately 60%, most of them between 75% and 90%, with differences between sMRI and fMRI, in favor of the second one (with accuracy peaks above 90%).

SVM is the most used technique, both for sMRI and fMRI, and could reach an accuracy close to 100% if combined with other ML techniques⁴² and the recent deep learning technique seems to be the most promising technique especially if it is used with structural and functional features together.^{46,48} Diverse inputs have been used to improve the accuracy of the technique: alterations in GM and WM (especially in sMRI studies), abnormalities in brain FC parameters (such as ReHo or density) and networks or the entire functional connectome. More brain areas have been evaluated, in particular the prefrontal (eg, DLPFC, orbitofrontal cortex), temporal and cingulate cortices, which seem to be the most helpful in predicting the diagnosis of SCZ, and insula that has been shown to have strong connection with aberrant activities in default mode in SCZ patients.

Significantly altered brain connectivity in patients with SCZ compared with HC can be efficiently detected by ML analysis (eg, DMN, visual network, sensorimotor network, frontoparietal network, SN, etc.). An integrated analysis using biomarkers from different types of biological sources (eg, fMRI, SNP) should be considered in order to improve the capacity to distinguish SCZ patients from HC and to facilitate diagnosis.

This systematic review has some limits to consider. Most studies had small sample sizes, and among these, only four of them enrolled drug-naïve patients, while all the others provided information about chronic patients under antipsychotic treatment; the great heterogeneity among the included studies may be a confounding element when interpreting the results. Moreover, no study compared drug-naïve SCZ patients with SCZ patients under treatment using ML methods applied to neuroimaging. This could be an interesting hint for future research. In

our systematic review, we only included papers about diagnostic discrimination on the basis of structural and functional neuroimaging features of HC vs SCZ patients, but the possible application of ML techniques should be considered in predicting individuals at risk, response to treatment and cognitive impairment; establishing disease phenotypes and in combining other data (ie, genetic analysis, EEG features, neuropsychological tests, serum biomarkers) to improve the accuracy of diagnosis. The work carried out by Guo et al²⁷ is the only study included in the review that also considered genetic susceptibility by comparing both patients with SCZ and their close relatives with HC; further research could aim at early diagnosis and reduction of confounding factors (eg, environmental risk factors) as far as possible. Another important aspect could be the high impact in terms of accuracy in discriminating chronic from acute patients. However, this application still seems to have too little impact in real life. In fact, it seems clear that it is easier to distinguish patients from HC than to distinguish patients from high-risk groups. Therefore, considering that all studies are based on patients already diagnosed with SCZ, either chronic or at their first episode, such applications still have a limited role in the real clinical field but could be extremely useful in distinguishing high-risk from low-risk patients in the future. The aim will, therefore, be to make ML more sophisticated in order to make not only categorical classifications but also dimensional diagnoses (eg, patients with prodromal symptoms of SCZ from HC).

Conclusion

In conclusion, the application of ML techniques will be useful to automatically classify patients with SCZ on the basis of structural and functional MRI. If systematically included in the diagnostic process of patients with SCZ, these techniques could help physicians to detect patients, even in the early stage of the disorder, conferring an important clinical advantage. We imagine that the greater accuracy demonstrated by the various predictive models illustrated in this systematic review and new models resulting from the integration of multiple ML techniques will be increasingly decisive in the future for the early diagnosis and evaluation of the treatment response and to establish the prognosis of patients with SCZ. To achieve a real benefit for patients, the future challenge is to reach an accurate diagnosis not only through the clinical evaluation but also with the aid of ML algorithms.

Abbreviation list

AOS, adolescent-onset schizophrenia; ASD, autism spectrum disorder; AUC, area under the ROC curve; BD, bipolar disorder; CoHe-ReHo, coherence regional homogeneity; DANS, discriminant autoencoder network with sparsity constraint; FNC, dynamic functional connectivity; DGM, deep neural generative model; DLPFC, dorso-lateral prefrontal cortex; DNN, deep neural network; DSM, Diagnostic and Statistical Manual of Mental Disorders; ELM, extreme learning machine ensembles; FC, functional connectivity; FES, first episode Schizophrenia; fMRI, functional magnetic resonance imaging; FNC, functional network connectivity; GM, grey matter; GMV, grey matter Volume; GPC, Gaussian process classifiers; HC, healthy controls; ICNs, intrinsic connectivity networks; L_0 norm, L_0 norm regularization; LASSO, Least Absolute Shrinkage and Selection Operator; LIBSVM, leave-one-out SVM; LOOCV, leave one out cross validation; MDD, major depressive disorder; ML, machine learning; MRI, Magnetic resonance imaging; MVPA, multivariate pattern analysis; N.A., not available; RFE, recursive feature elimination; ReHo, regional homogeneity; RF, random forest; LDA, linear discriminant analysis; ROC, receiver-operating characteristic curve analysis; rs-fMRI, resting state functional magnetic resonance imaging; ROI, region of interest; RVM, relevance vector machine; SCZ, schizophrenia; SN, salience network; SNPs, single-nucleotide polymorphisms; SRVS, sparse-representation-based variable selection; SVC, support vector classifier; SVM, support vector machine; VBM, voxel-based morphometry; V-ELM, voting-ELM; v-MKL, multiple kernel learning; WM, white matter.

Author contributions

All authors contributed to data analysis, drafting or revising the article, gave final approval of the version to be published, and agree to be accountable for all aspects of the work.

Disclosure

The authors report no conflicts of interest in this work.

References

1. Owen MJ, Sawa A, Mortensen PB. Schizophrenia. *Lancet*. 2016;388(10039):86–97. doi:10.1016/S0140-6736(15)01121-6

2. McGrath J, Saha S, Chant D, Welham J. Schizophrenia: a concise overview of incidence, prevalence, and mortality. *Epidemiol Rev*. 2008;30(1):67–76. doi:10.1093/epirev/mxn001
3. Simeone JC, Ward AJ, Rotella P, Collins J, Windisch R. An evaluation of variation in published estimates of schizophrenia prevalence from 1990–2013: a systematic literature review. *BMC Psychiatry*. 2015;15(1):193. doi:10.1186/s12888-015-0578-7
4. American Psychiatric Association. *Diagnostic and Statistical Manual of Mental Disorders*. 5th ed. Arlington (VA): American Psychiatric Association; 2013.
5. The ICD-10 classification of mental and behavioural disorders clinical descriptions and diagnostic guidelines. Available from: <http://www.who.int/classifications/icd/en/bluebook.pdf>. Accessed February 19, 2018.
6. Kambeitz J, Kambeitz-Ilanovic L, Leucht S, et al. Detecting neuroimaging biomarkers for schizophrenia: a meta-analysis of multivariate pattern recognition studies. *Neuropsychopharmacology*. 2015;40(7):1742–1751. doi:10.1038/npp.2015.22
7. Wolfers T, Buitelaar JK, Beckmann CF, Franke B, Marquand AF. From estimating activation locality to predicting disorder: A review of pattern recognition for neuroimaging-based psychiatric diagnostics. *Neurosci Biobehav Rev*. 2015;57:328–349. doi:10.1016/j.neubiorev.2015.08.001
8. Veronese E, Castellani U, Peruzzo D, Bellani M, Brambilla P. Machine learning approaches: from theory to application in schizophrenia. *Comput Math Methods Med*. 2013;2013:1–12. doi:10.1155/2013/867924
9. Vapnik VN. An overview of statistical learning theory. *IEEE Trans Neural Networks*. 1999;10(5):988–999. doi:10.1109/72.788640
10. Krystal JH, Murray JD, Chekroud AM, et al. Computational psychiatry and the challenge of schizophrenia. *Schizophr Bull*. 2017;43(3):473–475. doi:10.1093/schbul/sbx025
11. Liberati A, Altman DG, Tetzlaff J, et al. The PRISMA statement for reporting systematic reviews and meta-analyses of studies that evaluate health care interventions: explanation and elaboration. 2009;21(7):e1000100. doi:10.1371/journal.pmed.1000100
12. Jadad AR, Moore RA, Carroll D, et al. Assessing the quality of reports of randomized clinical trials: is blinding necessary? *Control Clin Trials*. 1996;17(1):1–12. Available from: <http://www.ncbi.nlm.nih.gov/pubmed/8721797>. Accessed November 22, 2017.
13. Salvador R, Radua J, Canales-Rodríguez EJ, et al. Evaluation of machine learning algorithms and structural features for optimal MRI-based diagnostic prediction in psychosis. Hu D, ed. *PLoS One*. 2017;12(4):e0175683. doi:10.1371/journal.pone.0175683
14. Lu X, Yang Y, Wu F, et al. Discriminative analysis of schizophrenia using support vector machine and recursive feature elimination on structural MRI images. *Medicine (Baltimore)*. 2016;95(30):e3973. doi:10.1097/MD.0000000000003973
15. Castellani U, Rossato E, Murino V, et al. Classification of schizophrenia using feature-based morphometry. *J Neural Transm*. 2012;119(3):395–404. doi:10.1007/s00702-011-0693-7
16. Xiao Y, Yan Z, Zhao Y, et al. Support vector machine-based classification of first episode drug-naïve schizophrenia patients and healthy controls using structural MRI. *Schizophr Res*. 2017. doi:10.1016/j.schres.2017.11.037
17. Greenstein D, Malley JD, Weisinger B, Clasen L, Gogtay N. Using multivariate machine learning methods and structural MRI to classify childhood onset schizophrenia and healthy controls. *Front Psychiatry*. 2012;3. doi:10.3389/fpsy.2012.00053
18. Pinaya WHL, Gadelha A, Doyle OM, et al. Using deep belief network modelling to characterize differences in brain morphometry in schizophrenia. *Sci Rep*. 2016;6(1):38897. doi:10.1038/srep38897
19. Pinaya WHL, Mechelli A, Sato JR. Using deep autoencoders to identify abnormal brain structural patterns in neuropsychiatric disorders: a large-scale multi-sample study. *Hum Brain Mapp*. 2019;40(3):944–954. doi:10.1002/hbm.24423

20. Iwabuchi SJ, Liddle PF, Palaniyappan L. Clinical utility of machine-learning approaches in schizophrenia: improving diagnostic confidence for translational neuroimaging. *Front Psychiatry*. 2013;4:95. doi:10.3389/fpsy.2013.00095
21. Cabral C, Kambeitz-Ilankovic L, Kambeitz J, et al. Classifying schizophrenia using multimodal multivariate pattern recognition analysis: evaluating the impact of individual clinical profiles on the neurodiagnostic performance. *Schizophr Bull*. 2016;42(suppl 1):S110–S117. doi:10.1093/schbul/sbw053
22. Chen X, Liu C, He H, et al. Transdiagnostic differences in the resting-state functional connectivity of the prefrontal cortex in depression and schizophrenia. *J Affect Disord*. 2017;217:118–124. doi:10.1016/j.jad.2017.04.001
23. Koch SP, Hägele C, Haynes J-D, Heinz A, Schlagenhauf F, Sterzer P. Diagnostic classification of schizophrenia patients on the basis of regional reward-related fMRI signal patterns. Schwarz AJ, ed. *PLoS One*. 2015;10(3):e0119089. doi:10.1371/journal.pone.0119089
24. Yoon JH, Tamir D, Minzenberg MJ, Ragland JD, Ursu S, Carter CS. Multivariate pattern analysis of functional magnetic resonance imaging data reveals deficits in distributed representations in schizophrenia. *Biol Psychiatry*. 2008;64(12):1035–1041. doi:10.1016/j.biopsych.2008.07.025
25. Reavis EA, Lee J, Wynn JK, et al. Assessing neural tuning for object perception in schizophrenia and bipolar disorder with multivariate pattern analysis of fMRI data. *Neuro Image Clin*. 2017;16:491–497. doi:10.1016/j.nicl.2017.08.023
26. Wang S, Zhan Y, Zhang Y, et al. Abnormal long- and short-range functional connectivity in adolescent-onset schizophrenia patients: a resting-state fMRI study. *Prog Neuropsychopharmacol Biol Psychiatry*. 2017;81:445–451. doi:10.1016/j.pnpbp.2017.08.012
27. Guo W, Liu F, Chen J, et al. Using short-range and long-range functional connectivity to identify schizophrenia with a family-based case-control design. *Psychiatry Res*. 2017;264:60–67. doi:10.1016/j.psychres.2017.04.010
28. Wang S, Zhang Y, Lv L, et al. Abnormal regional homogeneity as a potential imaging biomarker for adolescent-onset schizophrenia: a resting-state fMRI study and support vector machine analysis. *Schizophr Res*. 2017. doi:10.1016/j.schres.2017.05.038
29. Liu Y, Zhang Y, Lv L, Wu R, Zhao J, Guo W. Abnormal neural activity as a potential biomarker for drug-naive first-episode adolescent-onset schizophrenia with coherence regional homogeneity and support vector machine analyses. *Schizophr Res*. 2017. doi:10.1016/j.schres.2017.04.028
30. Chyzyk D, Savio A, Graña M. Computer aided diagnosis of schizophrenia on resting state fMRI data by ensembles of ELM. *Neural Netw*. 2015;68:23–33. doi:10.1016/j.neunet.2015.04.002
31. Zhu M, Jie N, Jiang T. Automatic classification of schizophrenia using resting-state functional language network via an adaptive learning algorithm. In: aylward S, Hadjiiski LM, eds. *Int Soc Opt Photonics*. 2014;9035:903522. doi:10.1117/12.2043240
32. Cao H, Duan J, Lin D, Shugart YY, Calhoun V, Wang Y-P. Sparse representation based biomarker selection for schizophrenia with integrated analysis of fMRI and SNPs. *Neuroimage*. 2014;102(Pt 1):220–228. doi:10.1016/j.neuroimage.2014.01.021
33. Yang H, Liu J, Sui J, Pearlson G, Calhoun VD. A hybrid machine learning method for fusing fMRI and genetic data: combining both improves classification of schizophrenia. *Front Hum Neurosci*. 2010;4:192. doi:10.3389/fnhum.2010.00192
34. Arbabshirani MR, Castro E, Calhoun VD. Accurate classification of schizophrenia patients based on novel resting-state fMRI features. *Conf Proc Annu Int Conf IEEE Eng Med Biol Soc Annu Conf*. 2014;2014:6691–6694. doi:10.1109/EMBC.2014.6945163
35. Chen H, Uddin LQ, Duan X, et al. Shared atypical default mode and salience network functional connectivity between autism and schizophrenia. *Autism Res*. 2017;10(11):1776–1786. doi:10.1002/aur.1834
36. Matsubara T, Tashiro T, Uehara K. Deep neural generative model of functional MRI images for psychiatric disorder diagnosis. *IEEE Trans Biomed Eng*. 2015;1-1. doi:10.1109/TBME.2019.2895663
37. Kim J, Calhoun VD, Shim E, Lee J-H. Deep neural network with weight sparsity control and pre-training extracts hierarchical features and enhances classification performance: evidence from whole-brain resting-state functional connectivity patterns of schizophrenia. *Neuroimage*. 2016;124(Pt A):127–146. doi:10.1016/j.neuroimage.2015.05.018
38. Watanabe T, Kessler D, Scott C, Angstadt M, Sripada C. Disease prediction based on functional connectomes using a scalable and spatially-informed support vector machine. *Neuroimage*. 2014;96:183–202. doi:10.1016/j.neuroimage.2014.03.067
39. Su L, Wang L, Shen H, Feng G, Hu D. Discriminative analysis of non-linear brain connectivity in schizophrenia: an fMRI study. *Front Hum Neurosci*. 2013;7:702. doi:10.3389/fnhum.2013.00702
40. Bae Y, Kumarasamy K, Ali IM, Korfiatis P, Akkus Z, Erickson BJ. Differences between schizophrenic and normal subjects using network properties from fMRI. *J Digit Imaging*. 2017. doi:10.1007/s10278-017-0020-4
41. Pläschke RN, Cieslik EC, Müller VI, et al. On the integrity of functional brain networks in schizophrenia, Parkinson's disease, and advanced age: evidence from connectivity-based single-subject classification. *Hum Brain Mapp*. 2017;38(12):5845–5858. doi:10.1002/hbm.23763
42. Liu Y, Guo W, Zhang Y, et al. Decreased resting-state interhemispheric functional connectivity correlated with neurocognitive deficits in drug-naive first-episode adolescent-onset schizophrenia. *Int J Neuropsychopharmacol*. 2018;21(1):33–41. doi:10.1093/ijnp/pyx095
43. Castro E, Gómez-Verdejo V, Martínez-Ramón M, Kiehl KA, Calhoun VD. A multiple kernel learning approach to perform classification of groups from complex-valued fMRI data analysis: application to schizophrenia. *Neuroimage*. 2014;87:1–17. doi:10.1016/j.neuroimage.2013.10.065
44. Qureshi MNI, Oh J, Cho D, Jo HJ, Lee B. Multimodal discrimination of schizophrenia using hybrid weighted feature concatenation of brain functional connectivity and anatomical features with an extreme learning machine. *Front Neuroinform*. 2017;11:59. doi:10.3389/fninf.2017.00059
45. Orban P, Dansereau C, Desbois L, et al. Multisite generalizability of schizophrenia diagnosis classification based on functional brain connectivity. *Schizophr Res*. 2017. doi:10.1016/j.schres.2017.05.027
46. Zeng -L-L, Wang H, Hu P, et al. Multi-site diagnostic classification of schizophrenia using discriminant deep learning with functional connectivity MRI. *EBio Med*. 2018;30:74–85. doi:10.1016/j.ebiom.2018.03.017
47. Amin MF, Plis SM, Chekroud A, et al. Reading the (functional) writing on the (structural) wall: multimodal fusion of brain structure and function via a deep neural network based translation approach reveals novel impairments in schizophrenia. *Neuroimage*. 2018;181:734–747. doi:10.1016/j.neuroimage.2018.07.047
48. Plis SM, Hjelm DR, Salakhutdinov R, et al. Deep learning for neuroimaging: a validation study. *Front Neurosci*. 2014;8. doi:10.3389/fnins.2014.00229

Neuropsychiatric Disease and Treatment

Dovepress

Publish your work in this journal

Neuropsychiatric Disease and Treatment is an international, peer-reviewed journal of clinical therapeutics and pharmacology focusing on concise rapid reporting of clinical or pre-clinical studies on a range of neuropsychiatric and neurological disorders. This journal is indexed on PubMed Central, the 'PsycINFO' database and CAS, and

is the official journal of The International Neuropsychiatric Association (INA). The manuscript management system is completely online and includes a very quick and fair peer-review system, which is all easy to use. Visit <http://www.dovepress.com/testimonials.php> to read real quotes from published authors.

Submit your manuscript here: <https://www.dovepress.com/neuropsychiatric-disease-and-treatment-journal>